ASSESSMENT OF CUMULUS PARAMETERIZATION SCHEMES IN MODELING METEOROLOGY ASSOCIATED WITH AN AIR POLLUTION EVENT IN THE ANDEAN REGION OF ECUADOR

RENE PARRA
Instituto de Simulación Computacional, Colegio de Ciencias e Ingeniería,
Universidad San Francisco de Quito, Ecuador

ABSTRACT

Air quality results from the interaction between emissions and meteorology. When significant changes occur, such as a sudden drop in temperature, atmospheric stability can persist, promoting air pollution. Between 7 and 9 November 2020, there was a significant drop in temperature in Cuenca (2,500 masl), a city located in the Andean zone in southern Ecuador. At noon, decreases of up to 700 W m^{-2} and 10°C were recorded in the solar radiation and temperature levels, respectively, compared to the first days of the month. At the same time, increments of around 20 µg m^{-3} in $PM_{2.5}$ hourly concentrations were recorded. Cumulus convection is a process directly related to cloud formation and, therefore, to solar radiation and temperature. We simulated the meteorology from 2 to 11 November 2020, with the Weather Research and Forecasting model (WRF 4.0.3), with a resolution of 1 km, without cumulus parameterization, and with nine options for this component. Modeling without this parameterization provided acceptable results for solar radiation and temperature. However, this option overestimated wind speed at the surface. Globally, option 10 (Kain–Fritsch Cumulus Potential) presented the best modeling performance. Options 3 (Grell–Freitas) and 6 (Tiedtke) were better or similar than modeling without cumulus parameterization. None of the options adequately modeled the temperature and solar radiation on 9 November 2020, the day on which the lowest values of these variables were observed, suggesting that the model will not provide proper values for days with sudden decreases in solar radiation and temperature. Because most parameterized effects, such as the boundary layer, convection, microphysics, and surface schemes, are closely linked, it is necessary to study their influence. It is also necessary to assess the potential benefit of data assimilation and even the development of dedicated schemes for numerical simulation in the equatorial zone of the Andes.

Keywords: Cuenca, cumulus convective, atmospheric forecasting, air quality forecasting, atmospheric stability.

1 INTRODUCTION

Air quality results from atmospheric emissions and meteorology [1]. When significant changes occur in atmospheric conditions, such as a sudden drop in temperature, atmospheric stability persists, and air pollution increases. The simulation of these events tests the performance of numerical models, which are expected to capture both meteorology and air quality. Air quality forecasting is crucial for reducing exposure and restricting anthropogenic sources during predicted periods of high pollution [2]. For this purpose, meteorological variables involved in atmospheric stability, like solar radiation, temperature, and wind speed at the surface, must be appropriately modeled.

Cumulus convection, which is typically parameterized, is a process directly related to cloud formation and, therefore, to solar radiation and temperature drops at the surface.

WIT Transactions on Ecology and the Environment, Vol 259,
www.witpress.com, ISSN 1743-3541 (on-line)
doi:10.2495/AWP220011

1.1 The air pollution event in Cuenca in November 2020

Between 2 and 11 November 2020, there was a substantial variation in cloudiness in Cuenca (2,500 masl), a city located in the Andean zone of southern Ecuador (Fig. 1). During 1–3 November (Sunday–Tuesday), there was little or no cloudiness, and in the following days, the atmosphere presented a partially or wholly cloudy cover (Fig. 2). On 9 November 2020 (Monday), the cloudiness was persistent. As consequence, decreases of up to 700 W m^{-2} and 10°C were recorded in the solar radiation and temperature levels at noon, respectively, compared to the previous days (Fig. 3). At the same time, the concentrations of primary pollutants increased. At the urban center, increments of around 20 µg m^{-3} in $PM_{2.5}$ hourly concentrations were recorded (Fig. 3).

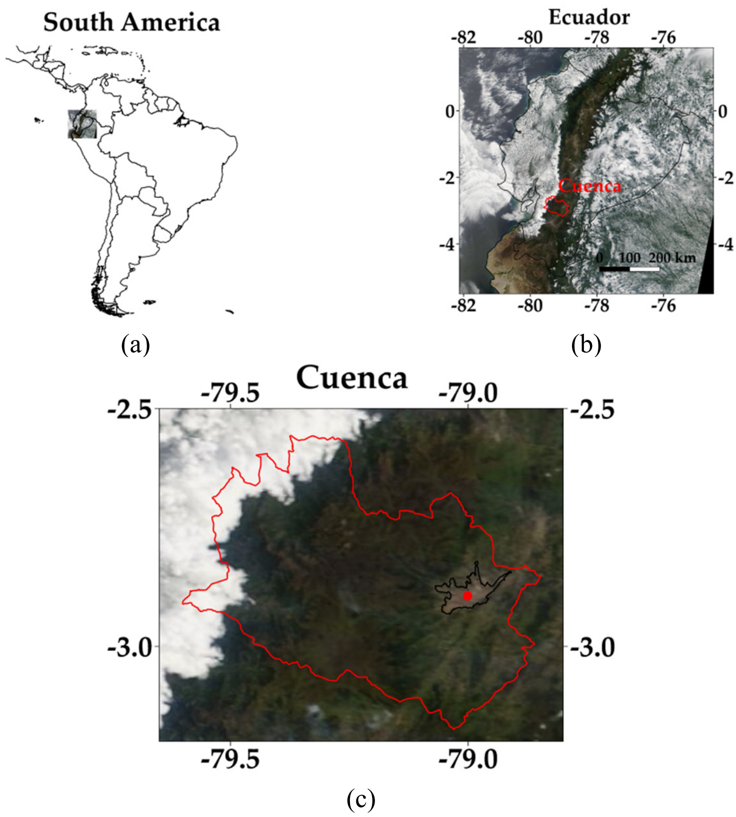

(a) (b) (c)

Figure 1: Location of: (a) Ecuador; and (b) Cuenca. (c) The urban area of Cuenca (black border) and MUN station (red dot, 2,500 masl). Satellite image corresponds to 3 November 2020 (Terra satellite, 10:30 LT) [5].

In the urban area of Cuenca, $PM_{2.5}$ emissions come mainly from vehicles that use diesel [3], [4]. Hourly emissions are typically higher during working days, and there are decreases on Saturdays, especially on Sundays, due to a lower flow of this type of vehicle. We did not identify the influence of other relevant sources during the study period. Fig. 3 indicates

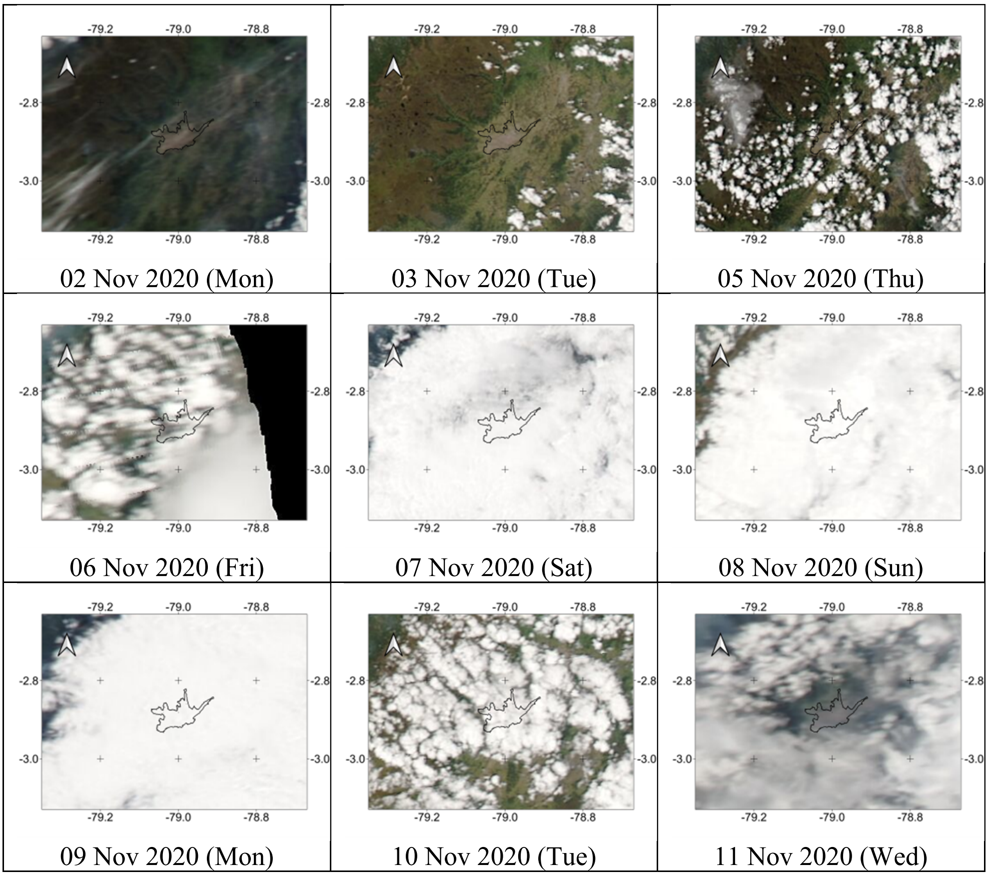

Figure 2: Satellite images from 2 to 11 November 2020 (Aqua satellite, 13:30 LT) [5]. The black border indicates the urban area of Cuenca.

maximum hourly concentrations of around 40 µg m^{-3} from 2 to 6 November (Monday to Friday) 2020. A drop in temperature is observed from 7 November (Saturday). On 9 November (Monday), the maximum temperature (15°C) was about 10°C lower than the previous weekdays. The maximum hourly concentration of $PM_{2.5}$ on Monday 9 November (60 µg m^{-3}) was 58% higher than the maximum hourly concentration on Monday 2 November (38 µg m^{-3}). If the $PM_{2.5}$ emissions were of the same magnitude on these two days, the difference in concentrations is explained by the more significant restriction of the atmosphere on 9 November to disperse the pollutants.

1.2 Modeling in the "grey zone"

Complex topography and land-use heterogeneity directly affect the atmospheric dynamic [6]. At 1 km of resolution, the topography representation of complex terrain improves. This benefit is significant for regions such as Cuenca. For this reason, atmospheric modeling was done using this spatial resolution for studying the influence of planetary boundary layer

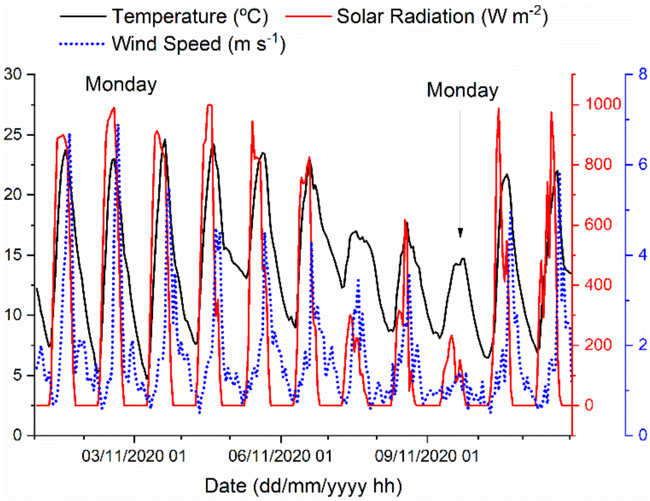

(a)

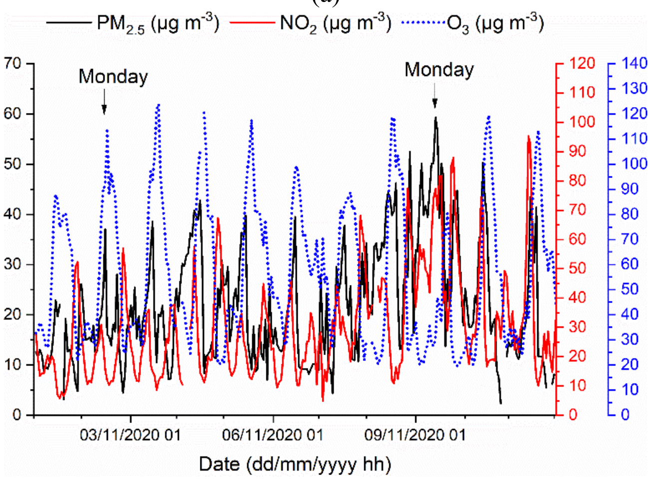

(b)

Figure 3: Records of the MUN station during 1 to 11 November 2020. (a) Meteorology; and (b) Air quality.

schemes in Cuenca [7], for assessing the influence on air quality due to the shift from diesel to electric buses [6], and the influence of feedback between aerosols and meteorology [8].

This horizontal grid spacing corresponds to the “grey zone”, a range of resolution in which phenomena such as turbulence, convective transport, and clouds are partly resolved, therefore, implying that might not be required modeling with cumulus convective parameterization [9]. Modeling in the grey zone is interesting to address whether working with higher resolution is always better [10].

As the length scale for convection (1 to 10 km) is similar to a spatial resolution of 1 km [9], this contribution explores the influence of cumulus parameterization schemes in modeling temperature, wind speed and solar radiation at the surface, from 2 to 11 November 2020, to address the following questions:

- What were the cumulus parameterization schemes with the best modeling performances?
- Is there a benefit when modeling without cumulus parameterization?
- Were the meteorological variables adequately modeled for 9 November 2020?

2 METHOD

2.1 Modeling approach

We used Weather Research and Forecasting (WRF version 4.0.3) [11] to model meteorology in Cuenca from 2 to 11 November 2020. Simulations were done through a master domain of 70 × 70 cells (27 km each) and three nested subdomains. The cells of the third domain (100 × 82) have 1 km of resolution and cover the region of Cuenca (Fig. 1(c)). Initial and boundary conditions were generated from the final NCEP FNL Operational Global Analysis data [12]. Table 1 summarizes the schemes and options selected for modeling. The variable "cu_physics" is used in WRF to select the cumulus parameterization options.

Table 1: Schemes and options for modeling meteorology in Cuenca (WRF 4.0.3) [13].

Component	**Option**	**Scheme/model**
Microphysics (mp_physics)	2	Purdue Lin
Longwave radiation (ra_lw_physics)	1	RRTM
Shortwave radiation (ra_sw_physics)	2	Goddard
Surface layer (sf_clay_physics)	1	Revised MM5
Land surface (sf_surface_physics)	1	5-layer thermal diffusion
Planetary boundary layer (bl_pbl_physics)	1	Yonsei University
Cumulus parameterization (cu_physics)	0 1 2 3 5 6 10 11 14 16	Without cumulus parameterization Kain–Fritsch Betts–Miller–Janjic, Janjic Grell–Freitas Grell–3D Tiedtke Kain–Fritsch–Cumulus potential Multi-scale Kain–Fritsch KIAPS SAS New Tiedtke

2.2 Metrics for modeling performance

Modeled hourly records of temperature and wind speed at the surface were assessed through the following metrics:

$$GE = \frac{1}{N}\sum_{i=1}^{N}|Pi - Oi|,\ BIAS = Pm - Om,\ RMSE = \sqrt{\frac{1}{N}\sum_{i=1}^{N}(Pi - Oi)^2}$$

$$IOA = 1 - \frac{\sum_{i=1}^{N}(Pi - Oi)^2}{\sum_{i=1}^{N}[|Pi - Pm| + |Oi - Om|]}$$

where GE = gross error; RMSE = root mean square error; IOA = index of agreement; N = number of values; Pm = mean modeled value; Om = mean observed value; Pi = modeled value; Oi = observed value. Table 2 indicates the benchmark values for these indicators.

Table 2: Metrics for meteorological modeling [14].

Parameter	Indicator	Benchmark
Hourly surface temperature	GE	< 2°C
	BIAS	< ±0.5°C
	IOA	≥ 0.8
Hourly wind speed at 10 m above the surface	RMSE	< 2 m s^{-1}
	BIAS	< ± 0.5 m s^{-1}
	IOA	≥ 0.6

In addition, modeled hourly values of global solar radiation at the surface were compared with records. For this variable, linear regressions (y = ax + b) were generated, corresponding x to records and y to computed values. In the case of a perfect fit, a and b variables will be 1 and 0, respectively, and the coefficient of determination (R^2) is equal to 1.

Records were provided by the MUN automatic station, which is located in the city's historic center (MUN station, Fig. 1(c)).

3 RESULTS AND DISCUSSION

Fig. 4 shows the hourly solar radiation records, temperature, wind speed at the surface, and the corresponding modeled values without cumulus parameterization (cu_physics = 0). Although their behaviors were captured by modeling, on 9 November 2020 they were overestimated. At 13:00 LT (9 November 2020), modeled solar radiation, temperature, and wind speed were up to 435 W m^{-2}, 5.5°C, and 1.1 m s^{-1} higher that the corresponding records. Similar patterns were obtained when modeling with cumulus parameterization (cu_physics = 1, 2, 3, 5, 6, 10, 11, 14, 16) (Fig. 5).

For the modeled period (2 to 11 November 2020), none of the cumulus options provided GE values for temperature into the benchmark range (GE < 2°C). The cumulus options with the lowest values for GE (2.2°C) were 0, 10, and 16 (Table 3). Options 0, 1, 3, and 10 provided the best BIAS values (–0.1 or 0.0°C) and into the benchmark range (< ±0.5°C). All the options provided IOA values higher than 0.8 (benchmark range). Options 1, 3, 10, and 16 provided the highest IOA values (0.90 or 0.91). Options 0 (no cumulus parametrization) and 10 showed the best metrics values for modeling the surface temperature.

Fig. 6 shows the observed and modeled wind speed values. The options reached RMSE values into the benchmark range (< 2 m s^{-1}) for wind speed. Options 1, 3, and 10 showed the best RMSE (1.1 m s^{-1}). Options 1, 3, 5, 6, 10, 11, and 14 provided the best BIAS values (–0.1, 0.0, or 0.1 m s^{-1}). All the options provided IOA values higher than 0.6 (benchmark range). Options 6, 10, and 14 obtained the highest IOA values (0.73 or 0.75). Options 6 and 10 showed the best metrics values for modeling the wind speed.

Options 1 and 10 obtained the best values for the linear regression between records and computed global solar radiation values (Table 3), with 0.79 to 0.80, 1.11, and 41.48 to 46.89 for R^2, a, and b, respectively. Options 0, 1, and 10 modeled better global solar radiation. Fig. 7 compares the records with modeled levels for the option without cumulus scheme. Even this option overestimated the solar radiation values on 9 November 2020.

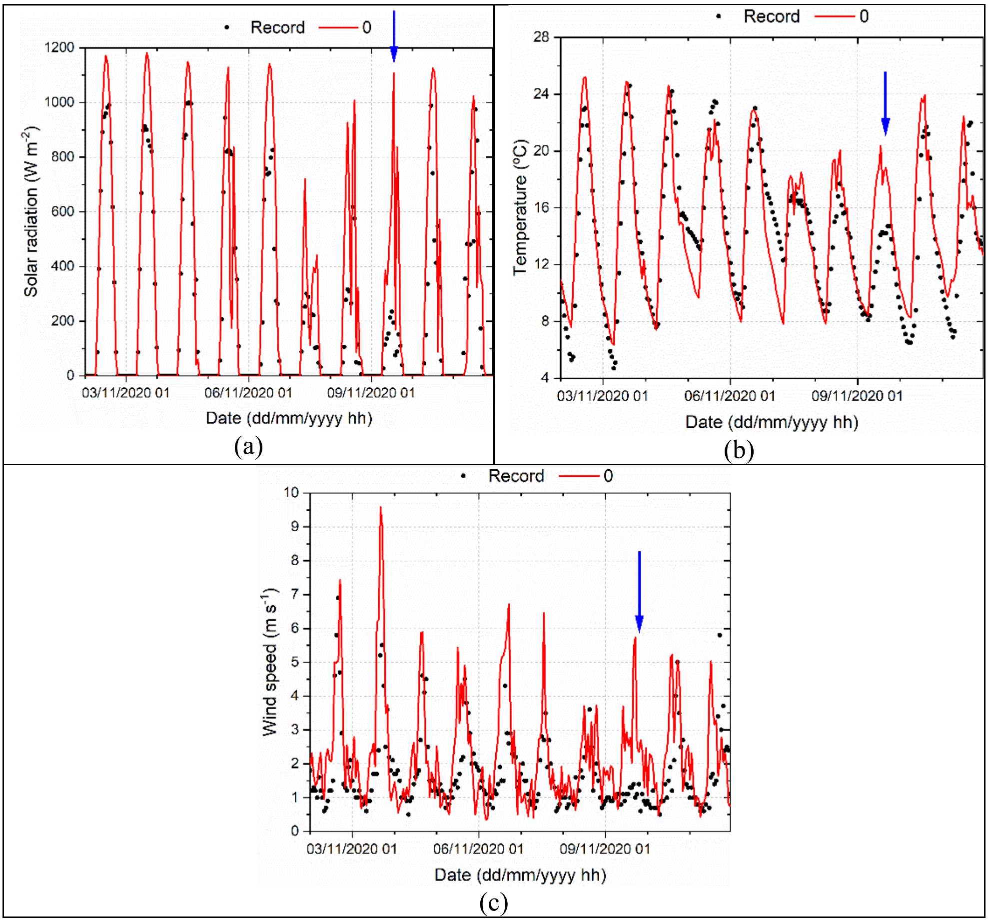

Figure 4: Observed and modeled values without cumulus parameterization (cu_physics = 0). (a) Solar radiation; (b) Temperature at the surface; and (c) Wind speed at 10 m above the surface. Blue arrow indicates midday on 9 November 2020.

Globally, option 10 (Kain–Fritsch Cumulus Potential [15]) presented the best modeling performance. This option replaces the ad hoc trigger function in the Kain–Fritsch cumulus parameterization (cu_physics = 1) with a trigger function related to the distribution of temperature and humidity in the convective boundary layer via probability density functions.

Options 3 (Grell–Freitas [16]) and 6 (Tiedtke [17]) were better or similar than modeling without cumulus parameterization. Option 3 is an improved Grell–Davenye scheme that tries to smooth the transition to cloud-resolving scales [13]. Option 6 is a mass-flux type scheme with convective potential energy removal, time scale, shallow component, and momentum transport.

None of the options adequately modeled the meteorological variables on 9 November 2020, the day on which the lowest values of solar radiation, temperature, and wind speed were observed during the studied period, suggesting that for forecasting purposes, none of

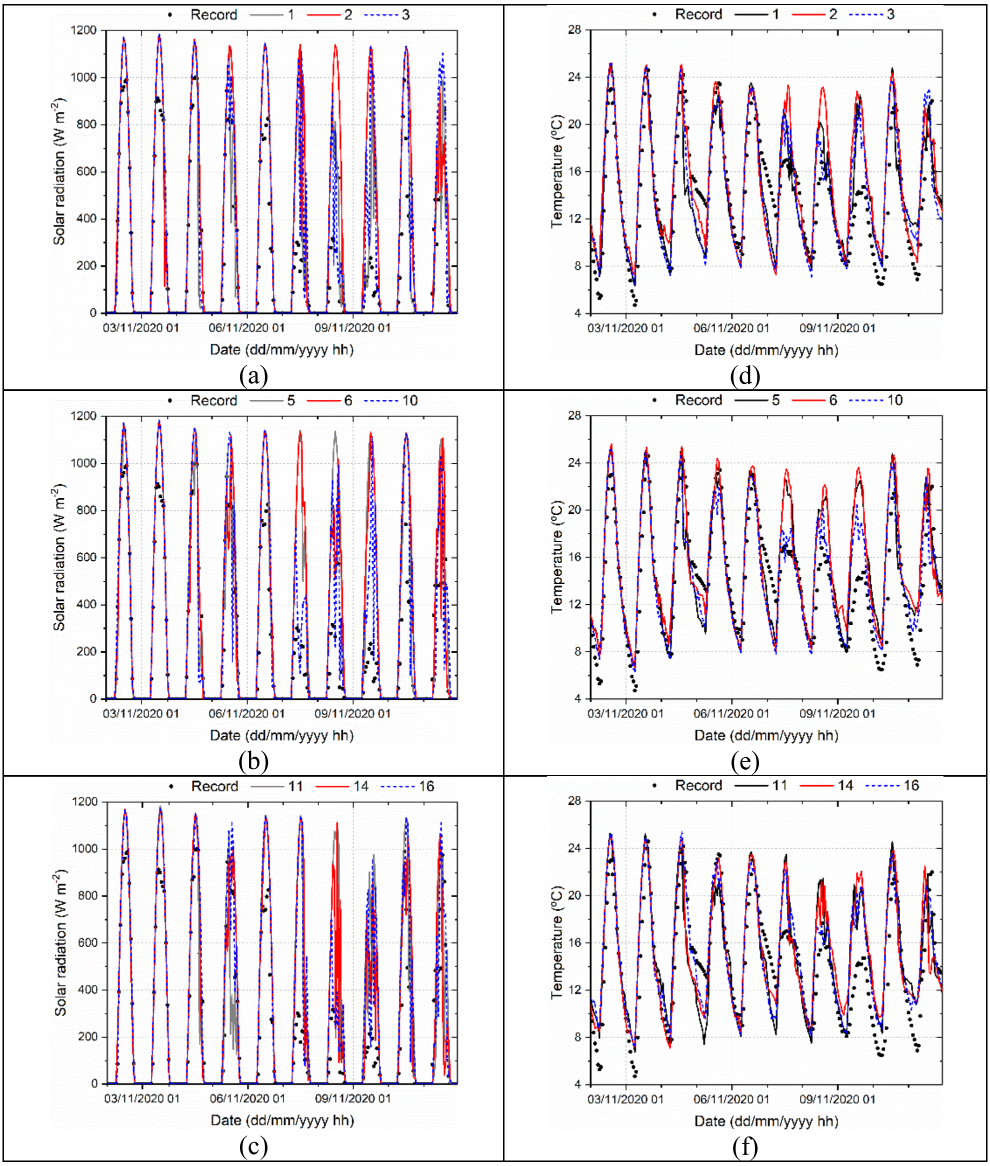

Figure 5: Observed and modeled values with different cumulus parameterization (cu_physics options: 1, 2, 3, 5, 6, 10, 11, 14, 16). (a), (b), (c) Solar radiation; and (d), (e), (f) Temperature.

the assessed cumulus options will provide proper values for days with significant drops in the magnitude of these parameters.

As 9 November 2020 was an overcast cloudiness day, its atmospheric stability corresponds to the neutral category D of the categories proposed by Pasquill [18]. The

Table 3: Metrics for meteorological modeling. Bold numbers fit the benchmark criterion. Numbers with grey background indicates the options with the best performances.

	Benchmark [14]	Cu_physics options									
		0	1	2	3	5	6	10	11	14	16
Hourly surface temperature:											
GE	< 2°C	2.2	2.4	2.5	2.4	2.5	2.6	2.2	2.6	2.5	2.2
BIAS	< ±0.5°C	**–0.1**	**0.0**	0.6	**–0.1**	0.6	0.8	**–0.1**	**0.3**	**0.4**	**0.4**
IOA	≥ 0.8	**0.91**	**0.89**	**0.88**	**0.90**	**0.88**	**0.88**	**0.91**	**0.88**	**0.88**	**0.91**
Hourly wind speed at 10 m above the surface:											
RMSE	< 2 m s^{-1}	**1.4**	**1.1**	**1.3**	**1.1**	**1.3**	**1.2**	**1.1**	**1.2**	**1.2**	**1.2**
BIAS	< ± 0.5 m s^{-1}	0.6	**–0.1**	**0.2**	**–0.1**	**0.0**	**0.1**	**–0.1**	**–0.1**	**0.0**	**–0.3**
IOA	≥ 0.6	**0.68**	**0.71**	**0.69**	**0.72**	**0.63**	**0.75**	**0.73**	**0.70**	**0.73**	**0.65**
Hourly solar radiation at surface:											
R^2	1.00*	0.79	0.80	0.73	0.78	0.69	0.73	0.79	0.69	0.72	0.77
a	1.00*	1.11	1.11	1.16	1.15	1.11	1.13	1.11	1.07	1.08	1.11
b	0.00*	48.34	41.48	83.23	52.49	82.19	79.52	46.89	66.57	63.07	54.46

*Values for perfect fitting.

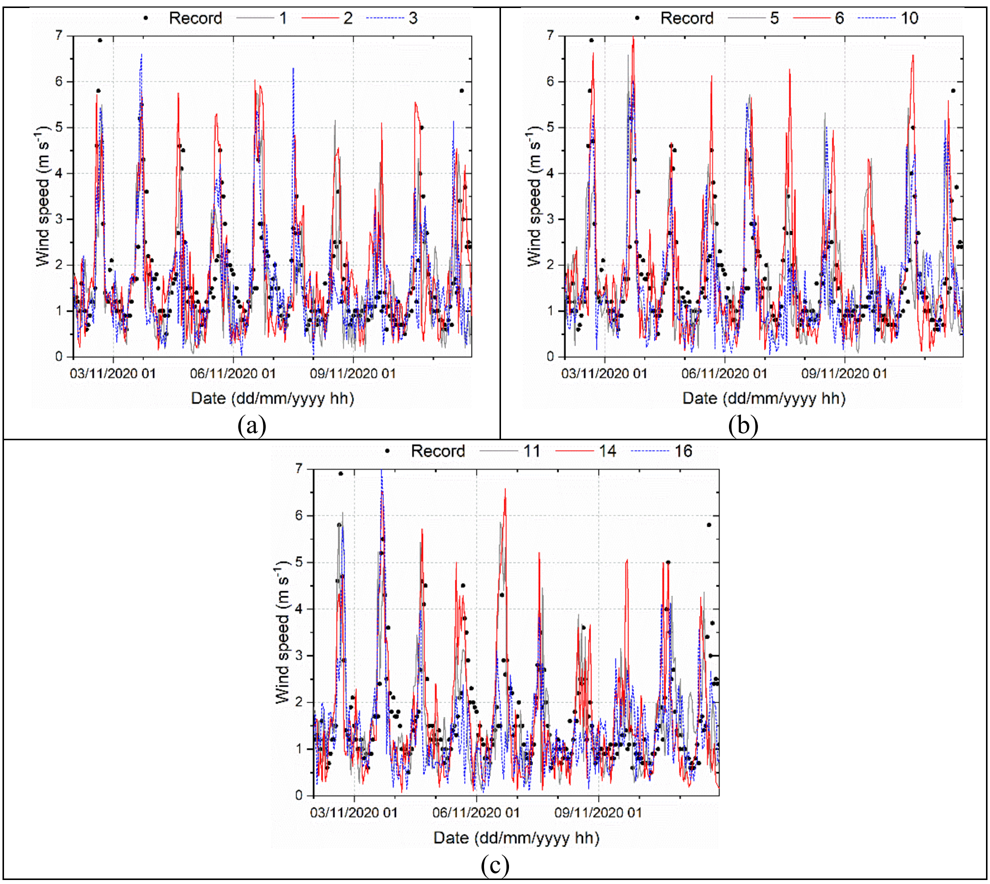

Figure 6: Observed and modeled wind speed values at 10 m above the surface, with different parameterization (cu_physics options: 1, 2, 3, 5, 6, 10, 11, 14, 16).

www.witpress.com, ISSN 1743-3541 (on-line)

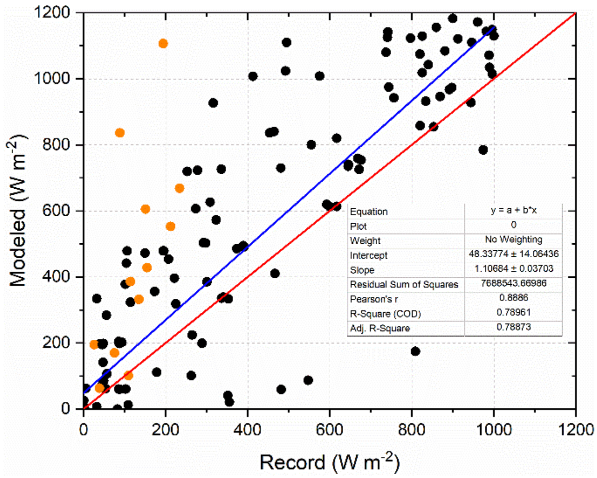

Figure 7: Observed and modeled (cu_physics = 0) solar radiation values at the surface. The red line corresponds to a perfect linear fit. The blue line indicates the linear fitting. The orange dots indicate the pairs of 9 November 2020.

modeled solar radiation and wind speed values at 13:00 LT with the cumulus option 10 were 696 W m^{-2} and 2.8 m s^{-1}, corresponding to the moderately unstable category B. Therefore, if these computed parameters were used for forecasting purposes, the computed $PM_{2.5}$ concentrations would be lower than records.

Models using spatial resolution smaller than 4 km are generally considered convection-permitting, and they do not rely on cumulus parameterization schemes [15], therefore, following the assumption that the model is able to resolve organized convection at this resolution. This assumption is congruent with Zhang et al. [19], who reported a clear improvement on modeling precipitation in the Central Great Plains, in the eastern Kansas and western Missouri region (USA), without using a cumulus scheme at a 4 km resolution. Even, Zhang et al. [19] concluded that the advantage of modeling without a cumulus scheme should become more evident with finer resolutions such as 1 km. However, our results indicated that modeling with a spatial resolution of 1 km requires dedicated assessment to verify the usefulness of cumulus parameterization for regions with a complex topography and land-use heterogeneity.

Because most parameterized effects, such as the boundary layer, convection, microphysics, and surface schemes, are closely linked, it is necessary to study the influence of these components in the future. Also, it is necessary to assess the potential benefit of data assimilation and even the development of dedicated schemes for numerical simulation in the equatorial zone of the Andes and model meteorology and air quality with feedback.

Wind direction is another meteorological parameter directly involved in the dispersion of air pollutants. Although this parameter has been acceptably modeled in Cuenca, e.g. [4], [7], it was not evaluated in this contribution and should be included in future studies.

4 CONCLUSIONS

None of the cumulus parameterizations assessed in this contribution adequately modeled the meteorological variables on 9 November 2020, the day the lowest values of solar radiation, temperature, and wind speed were observed from 2 to 11 November 2020. It suggests that none of the cumulus options will provide proper values for days with significant drops in the magnitude of these parameters for forecasting purposes. If the modeled meteorological variables were used with a proper emission inventory for air quality forecasting, this system would provide proper air quality concentrations, except on days with drops in meteorological parameters similar to the observed on 9 November 2020.

Results indicated that modeling with a spatial resolution of 1 km for regions with a complex topography and land-use heterogeneity requires dedicated assessment to verify the usefulness of cumulus parameterization. It should not be assumed that for simulations with this spatial resolution, by default, it is better to turn off the convective cumulus option.

ACKNOWLEDGEMENTS

This research is part of the project "Emisiones y Contaminación Atmosférica en el Ecuador 2021–2022" and was funded by the USFQ Poli-Grants 2021 – 2022. Simulations were done at the High Performance Computing system at the USFQ.

REFERENCES

[1] Baklanov, A. et al., Online coupled regional meteorology chemistry models in Europe: Current status and prospects. *Atmos. Chem. Phys.*, **14**(1), pp. 317–398, 2014.

[2] Kumar, R., Peuch, V.-H., Crawford, J.H. & Brasseur, G., Five steps to improve air-quality forecasts. *Nature*, **561**(7721), pp. 27–29, 2018.

[3] EMOV EP, Inventario de Emisiones Atmosféricas del Cantón Cuenca 2014, p. 88, 2016.

[4] Parra, R. & Espinoza, C., Insights for air quality management from modeling and record studies in Cuenca, Ecuador. *Atmosphere*, **11**(9), p. 998, 2020.

[5] EOSDIS Worldview, https://worldview.earthdata.nasa.gov/. Accessed on: 27 Feb. 2022.

[6] Chow, F., Schär, C., Ban, N., Lundquist, K., Schlemmer, L. & Shi, X., Crossing multiple gray zones in the transition from mesoscale to microscale simulation over complex terrain. *Atmosphere*, **10**(5), p. 274, 2019.

[7] Parra, R., Performance studies of planetary boundary layer schemes in WRF-Chem for the Andean region of southern Ecuador. *Atmospheric Pollution Research*, **9**(3), pp. 411–428, 2018.

[8] Parra, R., Effects of aerosols feedbacks in modeling meteorology and air quality in the Andean region of southern Ecuador. Santiago de Compostela, Spain, pp. 39–50, 2021. http://library.witpress.com/viewpaper.asp?pcode=AIR21-004-1. Accessed on: 28 Feb. 2022.

[9] Met Office, Grey zone project for model parameterizations. https://www.metoffice.gov.uk/research/approach/collaboration/grey-zone-project/index. Accessed on: 28 Feb. 2022.

[10] Kealy, J.C., Probing the "grey zone" of NWP: Is higher resolution always better? *Weather*, **74**(7), pp. 246–249, 2019.

[11] WRF, https://www2.mmm.ucar.edu/wrf/users/download/get_sources.html. Accessed on: 28 Jun. 2021.

[12] Research Data Archive, Commerce NC for EPWSSD of. NCEP FNL operational model global tropospheric analyses, continuing from July 1999. UCAR/NCAR, 2000. https://rda.ucar.edu/datasets/ds083.2/. Accessed on: 14 May 2021.

[13] WRF Users' Guide, https://www2.mmm.ucar.edu/wrf/users/docs/user_guide_v4/v4.0/contents.html. Accessed on 27 Feb. 2022.

[14] European Environment Agency, The application of models under the European Union's Air Quality Directive: A technical reference guide. LU Publications Office, 2011. DOI: 10.2800/80600.
[15] Berg, L.K., Gustafson, W.I., Kassianov, E.I. & Deng, L., Evaluation of a modified scheme for shallow convection: Implementation of CuP and case studies. *Monthly Weather Review*, **141**(1), pp. 134–147, 2013.
[16] Grell, G.A. & Freitas, S.R., A scale and aerosol aware stochastic convective parameterization for weather and air quality modeling. *Atmos. Chem. Phys*., **14**(10), pp. 5233–5250, 2014.
[17] Zhang, C., Wang, Y. & Hamilton, K., Improved representation of boundary layer clouds over the southeast Pacific in ARW-WRF using a modified Tiedtke cumulus parameterization scheme. *Monthly Weather Review*, **139**(11), pp. 3489–3513, 2011.
[18] De Visscher, A., *Air Dispersion Modeling: Foundations and Applications*, Wiley: USA, 634 pp., 2014. https://www.wiley.com/en-us/Air+Dispersion+Modeling%3A+Foundations+and+Applications-p-9781118078594. Accessed on: 4 Mar. 2022.
[19] Zhang, Y., Roundy, J.K. & Santanello, J.A., Evaluating the impact of model resolutions and cumulus parameterization on precipitation in NU-WRF: A case study in the Central Great Plains. *Environmental Modelling and Software*, **145**, 105184, 2021.